

LA-UR-01-6460

Approved for public release;  
distribution is unlimited.

*Title:* Validity and Limitations of the Three-Plane Compton Imaging  
Technique via Simulations

*Author(s):* Mohini W. Rawool-Sullivan, John P. Sullivan, James E. Koster, and  
Brian D. Rooney

*Submitted to:* Presented at the NSS/MIC 2001, San Diego, Ca, November  
2001 and submitted to IEEE transactions on nuclear science



Los Alamos National Laboratory, an affirmative action/equal opportunity employer, is operated by the University of California for the U.S. Department of Energy under contract W-7405-ENG-36. By acceptance of this article, the publisher recognizes that the U.S. Government retains a nonexclusive, royalty-free license to publish or reproduce the published form of this contribution, or to allow others to do so, for U.S. Government purposes. Los Alamos National Laboratory requests that the publisher identify this article as work performed under the auspices of the U.S. Department of Energy. Los Alamos National Laboratory strongly supports academic freedom and a researcher's right to publish; as an institution, however, the Laboratory does not endorse the viewpoint of a publication or guarantee its technical correctness.

# Validity and Limitations of the Three–Plane Compton Imaging Technique via Simulations

Mohini W. Rawool-Sullivan, John P. Sullivan, James E. Koster, and Brian D. Rooney

**Abstract--** At Los Alamos National Laboratory we are constructing a multi-layer prototype camera using Silicon pixel detectors. Each pixel detector is 5.80 cm × 6.30 cm × 200 microns. The pixels are 3 mm × 3 mm in size. With this prototype we intend to study electron tracking techniques along with the three–plane Compton imaging technique. In this paper we present results of the initial simulation studies of the three–plane Compton imaging technique using our prototype detector geometry for mono-energetic gamma sources with energies from 100 keV to 500 keV. The GEANT simulation package was used to carry out these studies.

## I. THE THREE-PLANE COMPTON IMAGING TECHNIQUE

To increase the efficiency of Compton imaging techniques [1]–[4] new detection concepts are being proposed. One such concept is a three–plane Compton imaging technique [5], [6]. This concept (Fig. 1) requires two successive Compton scatter interactions followed by a third interaction. All interactions must be in detectors with good spatial and energy resolution. In Fig. 1,  $E_\gamma$ ,  $E_2$ , and  $E_3$  are the incident photon energies for each interaction. The measured energy losses in each interaction are  $L_1$ ,  $L_2$ , and  $L_3$ , respectively. The Compton scatter angles for the first two Compton interactions are  $\Phi_1$  and  $\Phi_2$ , respectively. The two Compton equations then are,

$$\cos(\Phi_1) = 1 - mc^2 \left( \frac{1}{E_2} - \frac{1}{E_\gamma} \right) \quad (1)$$

$$\cos(\Phi_2) = 1 - mc^2 \left( \frac{1}{E_3} - \frac{1}{E_2} \right) \quad (2)$$

$$L_1 = E_\gamma - E_2 \quad (3)$$

$$L_2 = E_2 - E_3 \quad (4)$$

The angle  $\Phi_2$  is determined from the measured location of interactions in three separate interactions. Solving for  $E_\gamma$  in terms of measured quantities  $\Phi_2$ ,  $L_1$ , and  $L_2$  we get,

$$E_\gamma = L_1 + \frac{L_2}{2} + 0.5 * \left\{ L_2^2 + \frac{4mc^2 L_2}{1 - \cos(\Phi_2)} \right\}^{0.5} \quad (5)$$

Using the calculated value of  $E_\gamma$  along with the measured value of  $L_1$  and equation (1), the direction cone can be determined. With this concept, J. D. Kurfess et. al. [6], estimate that efficiencies as high as 25–50% could be reached in the MeV region. In this approach, background events will be discarded because the reconstruction of these background events will not lead to a valid Compton scattering sequence. We decided to test these equations for real-world situations by performing simple simulations. The incident photon energy range used in this paper is between 100 keV to 500 keV.

## II. SIMULATIONS

In this paper we review results of our simulation studies performed using the GEANT[7] Monte-Carlo package (version 3.21). This version of GEANT does not simulate the effect of Doppler broadening. Doppler broadening is important in the Compton scattering interaction[8] due to the fact that the gamma ray is not being scattered off of a free electron at rest. Instead, the electron is bound in an atom and has a finite momentum. This distributes the scattered gamma-ray energy about the energy predicted by the Compton equation. This effect degrades the energy resolution of the detector. The problem is worse for high-Z detectors, for which the momenta of inner shell electrons is higher. For Silicon (Si) and Germanium (Ge), the Doppler broadening of the Compton scattered gamma–ray energy is much larger than their intrinsic energy resolution. Thus, for these detectors the angular resolution due to energy uncertainty is dominated by Doppler broadening effects for incident energies above 500 keV in a single Compton scatter event[8]. For the 511 keV energy, the Doppler broadening effect in single Compton scattering off the Silicon was determined to be less than 3 keV (FWHM). For 1 MeV, this effect was determined to be less than 4.5 keV (FWHM)[8]. For future studies we intend to include Doppler broadening in our GEANT simulations

---

Manuscript received November 20, 2001.

M. W. Rawool-Sullivan is with the Los Alamos National Laboratory, Los Alamos, NM 87545 USA (telephone: 505-667-6628, e-mail: [mohini@lanl.gov](mailto:mohini@lanl.gov)).

J. P. Sullivan is with the Los Alamos National Laboratory, Los Alamos, NM 87545 USA (telephone: 505-665-5963, e-mail: [sullivan@lanl.gov](mailto:sullivan@lanl.gov)).

J. E. Koster is with the Los Alamos National Laboratory, Los Alamos, NM 87545 USA (telephone: 505-667-3346, e-mail: [jkoster@lanl.gov](mailto:jkoster@lanl.gov)).

B. D. Rooney is with the Los Alamos National Laboratory, Los Alamos, NM 87545 USA (telephone: 505-667-5372, e-mail: [rooney@lanl.gov](mailto:rooney@lanl.gov)).

package. However, for these studies we intended to look at the effects of our thin plane geometry only.

For our detector planes we chose Silicon pixel detectors with overall dimensions of  $5.80\text{ cm} \times 6.30\text{ cm} \times 200\text{ microns}$ . The pixels were  $3\text{ mm} \times 3\text{ mm}$  in size. We are currently constructing a three-layer prototype Silicon Compton camera of these dimensions to study the tracking of Compton-scattered-electrons. Therefore, we chose to simulate a detector corresponding to what we have in hand. Ideally, a detector with smaller pixels would be used for these studies. However, we wanted a detector with readout electronics attached to no more than two sides. This allows the prototype to be trivially scaled up laterally. The  $3\text{ mm}$  pixels on the prototype detector allowed us to use a “single-metal” design with readout on only two edges, which is cheaper and easier to build.

Although the three-plane Compton imaging technique only requires three planes, our simulation geometry included six planes separated by  $1\text{ cm}$  of air in between them. We used a six-plane geometry because we wanted to increase the probability of generating three-plane Compton events or events that will allow us to test the three-plane Compton imaging technique. A ‘real’ detector would probably include many more than six planes. Mono-energetic photon sources were used for these studies. As mentioned before, the incident energy range considered in these studies was from  $100\text{ keV}$  to  $500\text{ keV}$ . The output from our simulation program is written in ntuple [9] format. We store information such as energy deposited in each layer by primary and secondary particles, the number of “hits” (interactions that deposit energy in the active parts of the detector) in each layer, entrance and exit co-ordinates of each particle for all detector planes, particle identification number for each track, event number, GEANT run number, momentum of individual tracks, total energy (mass + kinetic energy) of each particle before and after interaction, path length (cm) in the individual Silicon detectors for the particles that caused a hit, and the time at which the particle entered the particular Si detector plane. A “good event” had a finite energy deposition ( $>1\text{ keV}$ ) in at least one of the Silicon detectors. Information from all “good events” was included in the output file. These output files were then analyzed using PAW [10]. This analysis searched for events with hits in at least three planes (called three-plane events). A subset of the original simulation information was saved for each of these three-plane events in another data file. In addition, the simulated hits were translated to pixel numbers and energy deposition or ADC values. Finally, this file containing three-plane events was analyzed with a third code that attempted to apply some of the equations above to the simulation results. When more than three planes were hit all combinations of three hit planes were analyzed.

Because the time differences between the hits in various Silicon layers ( $30\text{--}50\text{ ps}$ ) are generally much less than the expected time resolution of the detectors, the analysis algorithm cannot determine the time order in which the hits

took place. Therefore, the algorithm takes every combination of three hits in an event (e.g., six permutations when there are three hits in the event) and tries to reconstruct them as a three-plane Compton event. This algorithm uses only the information (pixel number, plane number, energy deposition value) that would be available in a “real” experiment.

In addition, the analysis of the three-plane Compton events looks at the information available only in a Monte Carlo (the time order of the hits, and the particle type that caused the hits, etc.) to count the number of events that contain two Compton scatterings and a third interaction by a photon. These are the events to which the equations above can be applied – the code counts the number of such events in the simulations. Three or more Silicon planes can also be hit by other processes. One possibly interesting example, is a Compton scattering that produces an electron with enough energy to hit three planes of Silicon. A count of such events is also kept.

### III. RESULTS

Fig. 2 shows a sample Compton scattered event from our simulations. This event is interesting in that an electron is produced in the second Silicon detector plane. After emerging from this plane, it passes through the third plane and ends up in the fourth plane. The multiple Coulomb scattering of the electron in the Silicon and in air (in between the detector planes) can be seen. In this event,  $23\text{ keV}$  is deposited in the second Silicon detector plane,  $208\text{ keV}$  in the third, and  $59\text{ keV}$  in the fourth Silicon detector plane. For this event the incident photon energy was  $500\text{ keV}$ . This event in the “real” experiment will appear as though it is a three-plane Compton event but will give a wrong value for  $E_\gamma$  and  $\Phi_1$ . This particular event points out one deficiency of using these equations in straightforward fashion in our detector geometry. Without use of additional measurements that will independently fix one of the parameters such as  $E_\gamma$  or without use of an algorithm that combines Monte-Carlo techniques and Compton scattering physics with experimental data, there is no way to positively determine which tracks constitute a valid three-plane Compton event scattering sequence in “real” experiments.

Fig. 3 shows the number of three-plane events per million incident photons for various incident photon energies. Open circles show events in which at least three Silicon detector planes had greater than  $1\text{ keV}$  deposited in them. The solid circles show the events with two Compton interactions followed by one other interaction that deposited at least  $1\text{ keV}$ . The open squares in the plot represent events in which the three or more Silicon detector planes had energy losses of at least  $1\text{ keV}$ , but the energy was deposited by a single Compton scatter electron (such as the one shown in Fig. 2). The data points labeled “3 plane Compton” and “3 planes by one e” events in Fig. 3 used information internal to the Monte Carlo. – That is this information could not easily be determined from experimental results. The intent is to show

the probability of three-plane Compton events occurring in our geometry. From Fig. 3, it is clear that the probability of an event in which three planes will have finite energy deposited is extremely low in our detector system. Although the probability of finding events in which three planes were hit goes up as the function of energy, the probability of finding the three-plane Compton events levels off. At 500 keV majority of the events in which three planes were hit are caused by Compton scattered electrons.

In Fig. 4 we have plotted the ratio of energy deposited in the Silicon detectors to the incident photon energy on the x-axis and the events on the y-axis for 100 keV (top), 300 keV (middle), and 500 keV (bottom) incident photon energies. While generating this plot, ‘perfect’ energy resolution (FWHM = 0 keV) was assumed and only events with “3 Si planes hit” were used. At 100 keV, a sharp peak is present in which all of the deposited energy is equal to the incident photon energy, i.e., a ratio of 1.0. The Compton edge for 100 keV is around 28 keV, or a ratio of 0.28 in Fig. 4. No sharp edge is seen at the Compton edge energy at 100 keV because three planes must have a finite energy loss to appear in this plot. The 28 keV electrons do not have enough energy to hit three Silicon detector planes. Therefore, multiple Compton and/or photoelectric interactions are needed for 100 keV incident photons. This eliminates the sharp Compton edge, but leaves the broad peak around ratio of 0.3.

At 300 keV the maximum electron energy from a single Compton scatter is 162 keV – again too low to hit three detector planes. Once again, a broad peak is seen around the ratio 0.54 corresponding to this maximum electron energy. The peaks just below a ratio of 1 are probably due to photoelectric interactions after which one or more Auger electrons or X-rays escaped from the Si. For 500 keV incident photons, the maximum electron energy rises to 331 keV. These electrons have enough energy to hit three planes. As a result, a sharp edge is seen at a ratio of 0.66, corresponding to a single Compton scatter in which the electron hits three planes. A small peak near a ratio of 1 is also seen. It is important to note here that it is not necessary to collect all of the incident photon energy in these three planes in the three-plane Compton imaging technique. Some energy may escape with the last photon (labeled  $E_4$  in Fig. 1), but the energy of the electron from the Compton scatters must be contained within the Silicon detector planes where the interaction took place

Since we had not included the Doppler effect in our simulations and we had assumed ‘perfect’ resolution, the broadening in these spectra can only be attributed to one or more of the following reasons:

1. Finite energy deposition was required which meant if the additional planes were hit with less than 1 keV of the energy, then that energy was not accounted for in our plot.
2. The possibility of multiple scattering in the air between detectors.

3. Inclusion of events where three planes were hit by single electrons.
4. Other three plane events where energy was lost to escaping electrons and/or gamma rays.

In Fig. 5 we have plotted the difference between calculated  $E_\gamma$  and incident photon energy used for respective simulations. For each event where three planes are hit, six permutations of time sequences are possible. For each sequence we calculated a value of  $E_\gamma$ . The “best” sequence was defined as the sequence for which the difference between the calculated  $E_\gamma$  and the sum of the energies deposited in the Silicon was minimum. Fig. 5 shows plots of the difference between calculated  $E_\gamma$  and incident photon energy from the “best” sequences of three-plane events for 100 keV (top), 300 keV (middle), and 500 keV (bottom). The plot at 100 keV shows a sharp peak at the difference of zero. At 500 keV, such a peak at zero is non-existent.

#### IV. DISCUSSION

One problem contributing to the relatively small probability for three-plane Compton events in these simulations is the detector design used in these simulations. Our detector was designed for tracking the electrons generated in a Compton interaction. In the three-plane Compton imaging technique the validity of equations (1) through (5) depends on the following necessary conditions.

- The first two interactions must be Compton interactions.
- The energy deposited in the first and second Compton interactions ( $L_1$  and  $L_2$ ) must be equal to the kinetic energy of the Compton-scattered electron. That is the Compton scattered electron in each of these interactions must lose all of its energy in the detector plane where the Compton interaction takes place.

These conditions require detector planes thick enough to stop the Compton-scattered electrons generated within the plane. Fig. 6 shows the CSDA (continuous-slowing-down approximation) range<sup>1</sup> of electrons in  $\mu\text{m}$  (microns) as a function of electron energy in keV. The range data used in this plot were obtained from ESTAR database [11]. The range data in Fig. 6 are the total range of the electron. Due to multiple scattering, the practical range of the electron is somewhat lower. As seen in Fig. 6, electrons of energy

---

<sup>1</sup> The CSDA range is a very close approximation to the average path length traveled by an electron particle as it slows down to rest, calculated in the continuous-slowing-down approximation. In this approximation, the rate of energy loss at every point along the track is assumed to be equal to the same as the total stopping power. Energy-loss fluctuations are neglected. The CSDA range is obtained by integrating the reciprocal of the total stopping power with respect to energy.

around 175 keV range out in the 200-micron-thick Silicon. Around 300 keV incident gamma ray energy the Compton edge corresponds to approximately 175 keV. Thus, for incident photon energies above 300 keV, a large fraction of Compton-scattered electrons escape from the Silicon detector planes in our simulations -- giving erroneous information on the energy deposited ( $L_1$  and  $L_2$ ) in the detector. In addition, these escaped electrons sometimes appear to be three-plane Compton events -- as in the sample event shown in Fig. 2. Also, in Fig. 3 a very rapid rise in the probability for three planes to be hit by one electron starts around  $E_\gamma = 300$  keV. At  $E_\gamma \approx 440$  keV, the maximum electron energy is high enough to pass through two Silicon detectors (400 microns).

Clearly, the desire for thicker detectors to stop the electrons is in conflict with the desire for thinner detectors that limits the photons to one Compton interaction per plane. The first two Compton scatterings and the third interaction must be in separate detector planes in order to measure the angle  $\Phi_2$  accurately. These conflicting thickness requirements result in an optimal thickness that increases with the incident photon energy of interest. Although current thickness of our Silicon detector planes is acceptable for up to 300 keV incident photon energy, a thicker Silicon detector is clearly better even in the 100-300 keV range. In this work, we have tried to study an existing detector system -- in which the detector thickness is not ideal for the three-plane Compton technique.

## V. REFERENCES

- [1] V. Schonfelder, A. Hirner, and K. Schneider, "A telescope for soft gamma-ray astronomy," *Nucl. Instr. Meth.*, Vol. 107, pp. 385-394, 1973.
- [2] M. Singh, "An electronically-collimated gamma camera for SPECT. Part I: Theoretical considerations and design criteria," *Med. Phys.*, Vol 10, pp. 421-427, 1983.
- [3] J. B. Martin, N. Dogan, J. E. Gormley, G. F. Knoll, M. O'Donnell, and D. K. Wehe, "Imaging Multi-Energy Gamma-Ray Fields With a Compton Scatter Camera," *IEEE Trans. Nucl. Sci.* Vol. 41, No. 4, pp. 1019-1025, 1994.
- [4] S. E. King; G. W. Phillips, P. S. Haskins, J. E. McKisson, R. B. Piercey, R. C. Mania, "A solid-state Compton camera for three-dimensional imaging," *Nucl. Instr. Meth. A*, Vol. 353, pp. 320-323, 1994.
- [5] N. Dogan, "Multiple Compton Scatter Camera for Gamma-ray imaging," Ph. D. dissertation, University of Michigan, Ann Arbor, MI, 1993.
- [6] J. D. Kurfess, W. N. Johnson, R. A. Kroeger, and B. F. Philips, "Considerations for the Next Compton Telescope Mission." *Proc. AIP Conf.*, 2000, 510, pp. 789-793.
- [7] Applications software group, "GEANT: Detector Description and Simulation Tool," *CERN Program Library Long Write-up W5013*, CERN, Geneva, Switzerland, 1993.
- [8] Y. F. Du, Z. He, G. F. Knoll, D. K. Wehe, W. Li, "Evaluation of a Compton scattering camera using 3-D position sensitive CdZnTe detectors," *Proc. SPIE*, 1999, Vol. 3768, pp 228-238.
- [9] Information technology division, "HBOOK -- Statistical Analysis and Histogramming," *CERN Program Library Long Write-up Y250*, CERN, Geneva, Switzerland 1995-1998.
- [10] Information technology division, "PAW: Physics Analysis Workstation, User's Guide," *CERN Program Library Long Write-up Q121*, 1992-1999.
- [11] M. J. Berger, J. S. Coursey, and M. A. Zucker, (1999), "ESTAR, PSTAR, and ASTAR: Computer Programs for Calculating Stopping-

Power and Range Tables for Electrons, Protons, and Helium Ions," (version 1.21), [Online]. Available: <http://physics.nist.gov/Star> [2001, November 16]. National Institute of Standards and Technology, Gaithersburg, MD.

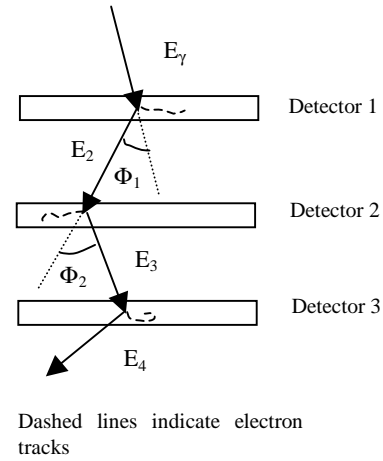


Fig. 1: Schematic Diagram of the Three-plane Compton Imaging Technique.

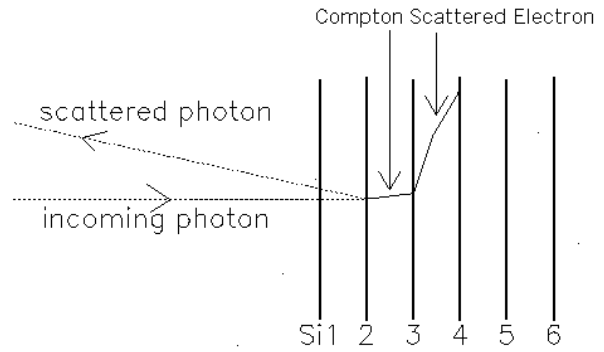


Fig. 2: Sample Compton-scattered event from GEANT. Air fills the space between and around the detectors.

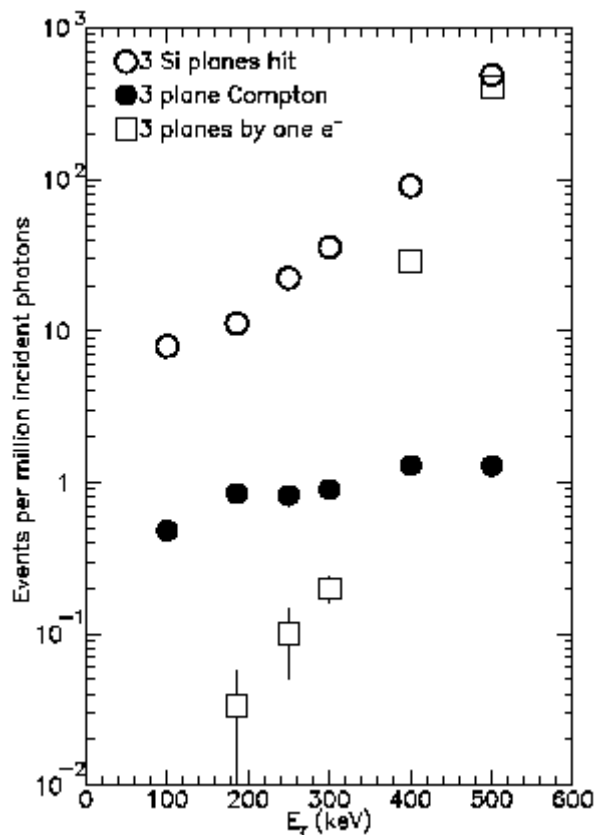


Fig. 3. Three plane events per incident photon energy. There are no “3 planes by one  $e^-$ ” events at 100 keV (from 200 million incident photons).

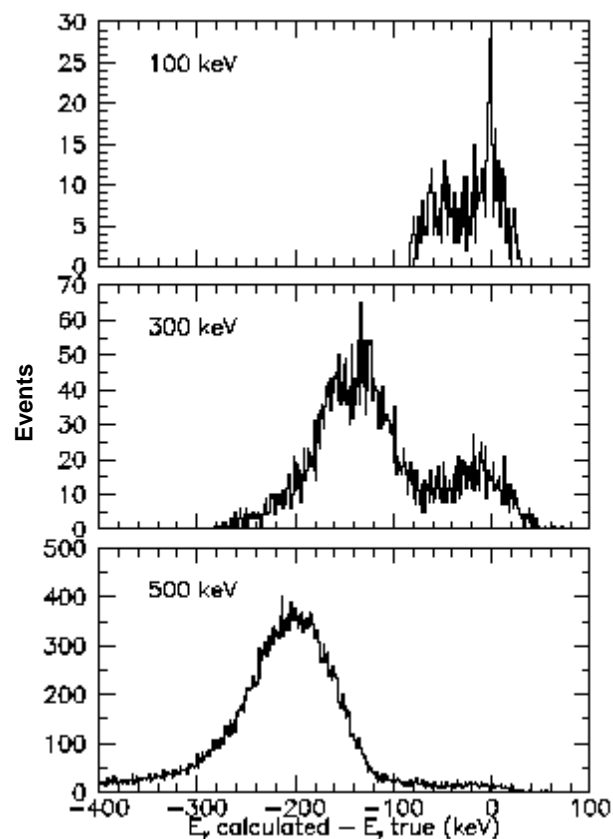


Fig. 5. Difference between calculated and true incident photon energy at 100 keV, 300 keV and 500 keV.

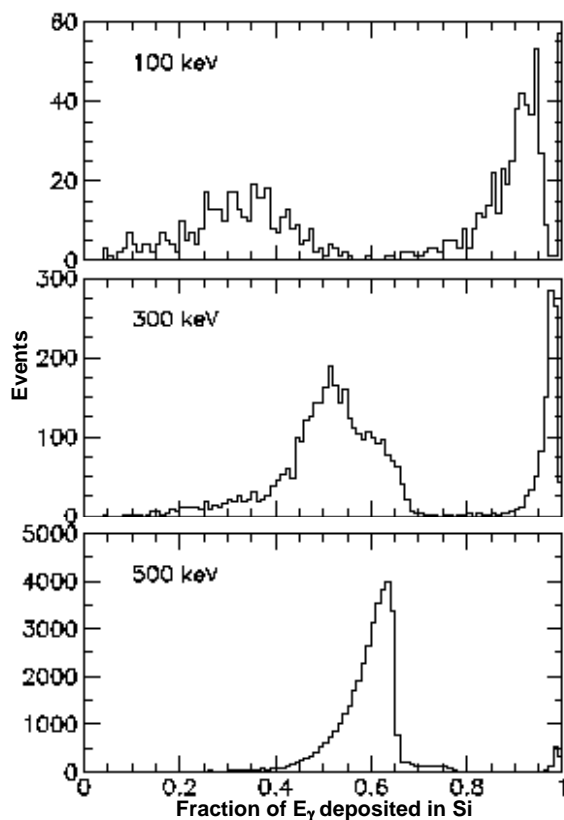


Fig. 4. Fraction of total  $E_\gamma$  deposited in Silicon for three-plane events. Y axis represents events.

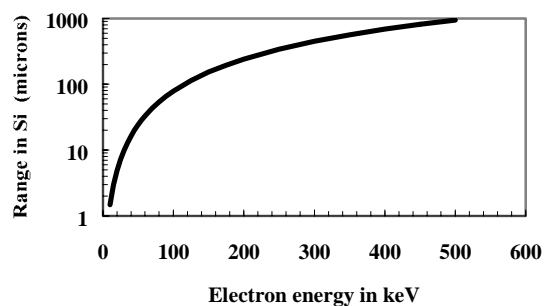


Fig. 6: Range curve for electrons in Silicon